International Journal of High-Rise Buildings
December 2019, Vol 8, No 4, 303-311
https://doi.org/10.21022/IJHRB.2019.8.4.303

International Journal of
High-Rise Buildings
www.ctbuh-korea.org/ijhrb/index.php

Wind-induced Aerodynamic Instability of Super-tall Buildings with Various Cross-sectional Shapes

Wonsul Kim[1†], Akihito Yoshida[2], and Yukio Tamura[2,3]

[1]*Research Institute for Infrastructure Performance, Korea Infrastructure Safety Corporation, Jinju, Korea*
[2]*Wind Engineering Research Center, Tokyo Polytechnic University, Atsugi, Japan*
[3]*School of Civil Engineering, Chongqing University, Chongqing, China*

Abstract

The effectiveness of aerodynamic modification to reduce wind loadings has been widely reported. However, most of previous studies have been investigated dynamic forces and pressure distributions on tall buildings with various unconventional configurations. This study was investigated dynamic characteristics and aerodynamic instability of super-tall buildings with unconventional configurations through extensive aeroelastic model experiments. Seventeen types of super-tall building models were considered such as basic and corner modification with corner cut, chamfered, oblique opening, tapered, inversely tapered, bulged, helical with twist angles of 90°, 180°, 270°, 360° and composite with 360° helical & corner cut, 4-tapered & 360° helical & corner cut, setback & corner cut, setback & 45° rotate. As a result, aerodynamic characteristics of helical models with single modification are superior to those of other models with single modification. However, effect of twist angle for helical model is negligible. Further, the 4-tapered & 360°helical & corner cut model is most effective in reducing the along- and across-wind fluctuating displacement responses in all of experimental models.

Keywords: Aerodynamic instability, Super-tall building, Wind-induced vibration, Aero-elastic model experiment, Aerodynamic damping

1. Introduction

Super tall buildings have been constructed in many cities around world for the enhancement of city competiveness and city image improvements despite an economic depression for many years. Tamura et al. (2011) reported the world skyscrapers under construction as January 2010. 56% of those within the top 100 highest buildings had been completed since 2000, and many tall buildings higher than 600 m are still under construction. Tall buildings have been generally designed to be symmetric rectangular, triangular or circular in plan, to avoid excessive seismic torsional vibrations due to eccentricity. However, freewheeling building shapes have advantages in structural design reducing wind loads. Particularly across-wind response which is a major factor in safety and habitability of tall buildings is greatly suppressed. The effectiveness of aerodynamic modification for super-tall buildings with various unconventional configurations to reduce wind loads has been widely reported for several decades (Bandi et al., 2013, Cooper et al., 1997, Davenport, 1988, Kawai, 1998, Kim and Kanda, 2010, Kim et al., 2011, Kim et al., 2002, Kwork et al., 1988, Tanaka et al., 2013, Tanaka et al., 2012). However, most of the above papers have focused on aerodynamic characteristics through the high-frequency force balance experiment and pedestrian level wind around tall buildings with various unconventional configurations.

In this study, extensive aeroelastic model experiments for super-tall buildings with various unconventional configurations were conducted to investigate the wind-induced response characteristics and aeroelastic instability of super-tall buildings with various unconventional configurations.

Corresponding author: Wonsul Kim
Tel: +82-55-771-4645; Fax: +82-55-771-4939
E-mail: wskim@kistec.or.kr

2. Wind Tunnel Experiments

2.1. Experimental models

Seventeen types of the super-tall building models are considered in this study as shown in Figure 1.

Table 1 lists the dynamic properties of super-tall building models. As shown in Table 1, the full-scale height and the moment of inertia of each building models are commonly set at H = 400 m (80 stories) and 9.03×10^{12} kgm^2.

The represent width and breadth are same with 50 m, and the aspect ratio H/(BD)$^{1/2}$ is 8. The first mode natural frequency of the full-scale model is assumed as 0.1 Hz and structural damping ratio is set at 0.01. The geometric scale of the experimental models is set at 1/1000 by a limit of the mass ratio as shown in Table 1.

2.2. Simulated natural wind

The aeroelastic model experiments are performed in a closed-circuit-type boundary layer wind tunnel whose

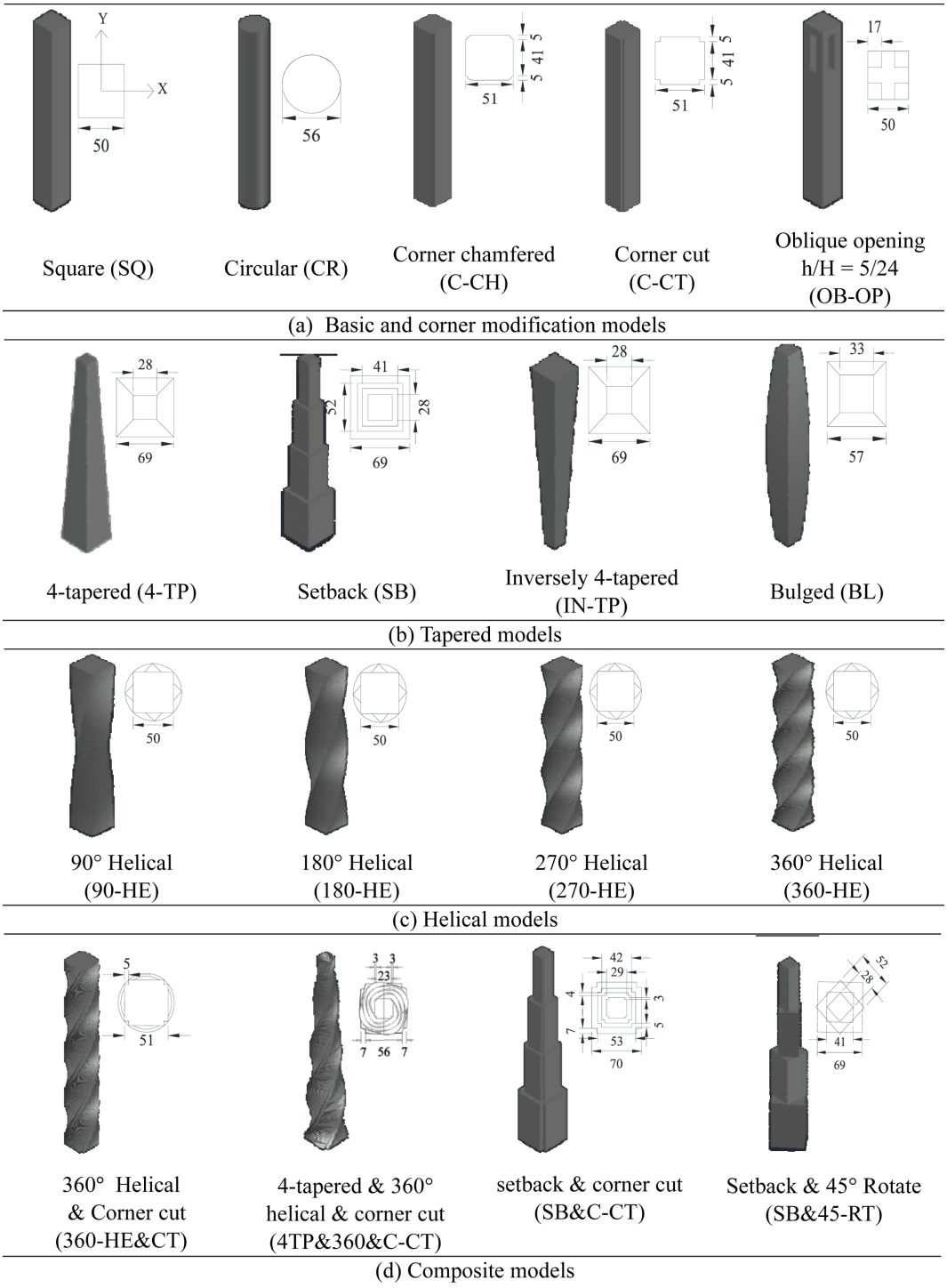


Figure 1. Super-tall building models.

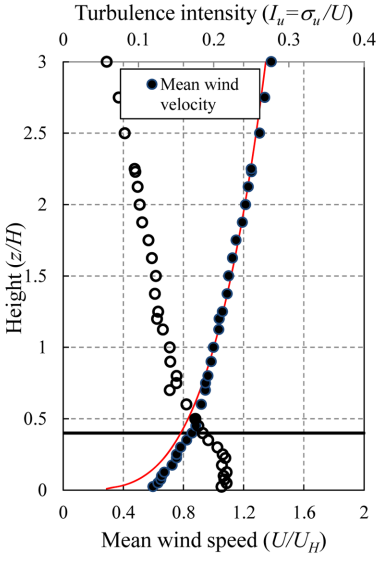
working section is 2.2 m wide, 1.8 m high, and 19 m long. In this study, the flow of the atmospheric boundary layer in the wind tunnel was interpreted on a geometrical scale of approximately 1/1000. Using the spire-roughness technique with a power lay exponent of 0.27, the approach flow was determined to represent an urban wind exposure corresponding to AIJ Recommendations for Loads on Buildings (AIJ-RLB 2004). The wind velocity and turbulence intensity at the topmost point of the model in the wind tunnel were about 8.86 m/s and 14%, respectively, as shown in Figure 2(a). The power spectrum density of the fluctuating wind velocity as a function of the turbulence length scale is presented in Figure 2(b).

2.3. Aeroelastic model experiment

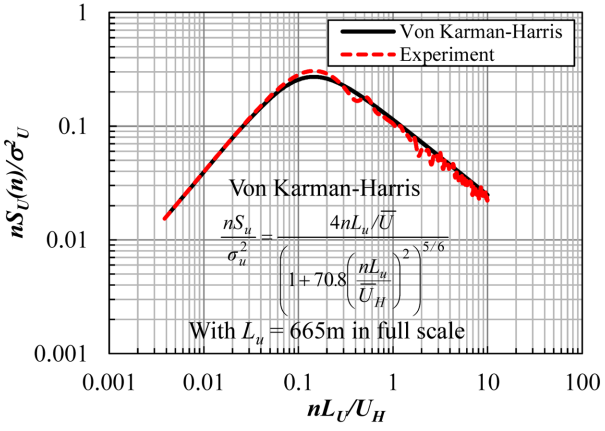
The aeroelastic model experiment requires scaling of the

Table 1. Dynamic properties of super-tall building models

	Height (m)	Moment of inertia $I_{x,y}$ (kg·m^2)	Natural frequency (Hz)	Ave. structural damping ratio (%)	Model scale λ_m	Velocity scale λ_v	Design Wind speed (m/s)
Prototype	400	9.03×10^{12}	0.1	1.0	1/1	1/1	62.4
Square	0.4	0.00919	13.489	1.1	1/1000	1/7.4	8.4
Circular	0.4	0.00937	11.627	1.0	1/1000	1/8.5	7.3
Corner Chamfered	0.4	0.00889	14.160	1.07	1/1000	1/7.1	8.1
Corner Cut	0.4	0.00895	14.886	1.1	1/1000	1/6.8	9.2
Oblique opening h/H = 5/24	0.4	0.00914	11.187	1.0	1/1000	1/8.9	7.0
90° Helical	0.4	0.00909	12.512	1.15	1/1000	1/8.0	7.8
180° Helical	0.4	0.00887	12.329	1.27	1/1000	1/8.1	7.7
270° Helical	0.4	0.00866	12.451	1.15	1/1000	1/8.0	7.8
360° Helical	0.4	0.00887	12.329	1.11	1/1000	1/8.1	7.7
360° Helical & Corner Cut	0.4	0.00907	11.108	1.03	1/1000	1/9.0	6.9
4-Tapered	0.4	0.00896	12.268	1.10	1/1000	1/8.1	7.7
Inverse tapered	0.4	0.00875	11.902	1.00	1/1000	1/8.4	7.4
Setback	0.4	0.00904	11.841	1.06	1/1000	1/8.4	7.4
Bulged	0.4	0.00887	11.779	1.14	1/1000	1/8.5	7.3
4-Tapered & 360° Helical & Corner Cut	0.4	0.00857	11.597	1.06	1/1000	1/8.7	7.2
Setback & Corner cut	0.4	0.00930	11.291	1.14	1/1000	1/8.9	7.0
Setback & 45° Rotate	0.4	0.00909	11.536	1.06	1/1000	1/8.7	7.2



(a) mean wind speed and turbulence intensity profiles



(b) Power spectral density of fluctuating wind velocity at model height

Figure 2. Simulated natural wind in wind tunnel.

dynamic properties (mass, stiffness, and frequency) of a building in the fundamental sway modes based on the similarity theory. Figure 3 shows experimental model and gimbal system of the aeroelastic model experiment. The experimental model which is rigid model was composed of a gimbal which rotated freely with respect to the X-Y axes, a coil spring which provided stiffness and magnetic damper which provided damping, all mounted on a base of supporting structure. First mode frequency was adjusted by additional mass installed in the top of the model. Further, to avoid noise from outside and forced vibration of the base, the support system has been completely separate from the wind tunnel. To measure displacements in X- and Y-directions, two laser displacement transducers were installed as shown in Figure 3.

The design wind velocity at the building height was 62.41 m/s, and the wind velocity scale was 1/7.5. The wind velocity was considered from 0 to 12.5 m/s which is about 1.35 times from the design wind speed. The wind direction was only considered 0 at which maximum response is

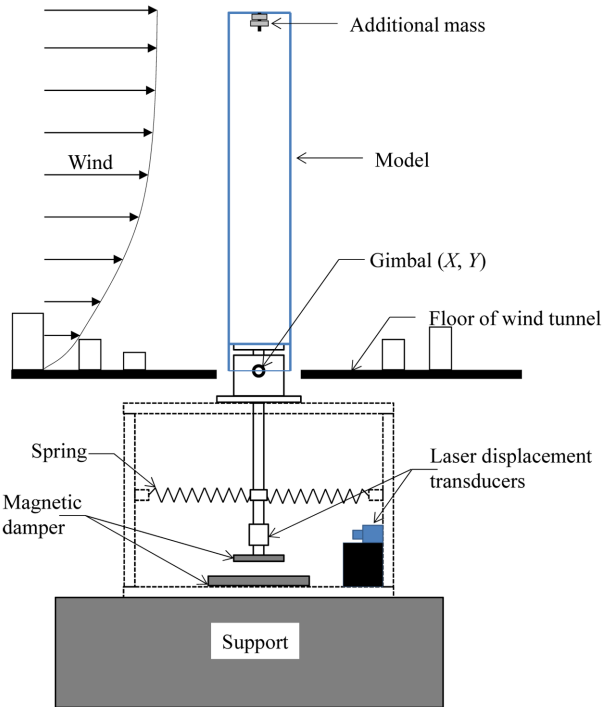


Figure 3. Gimbal system of the aeroelastic model experiment.

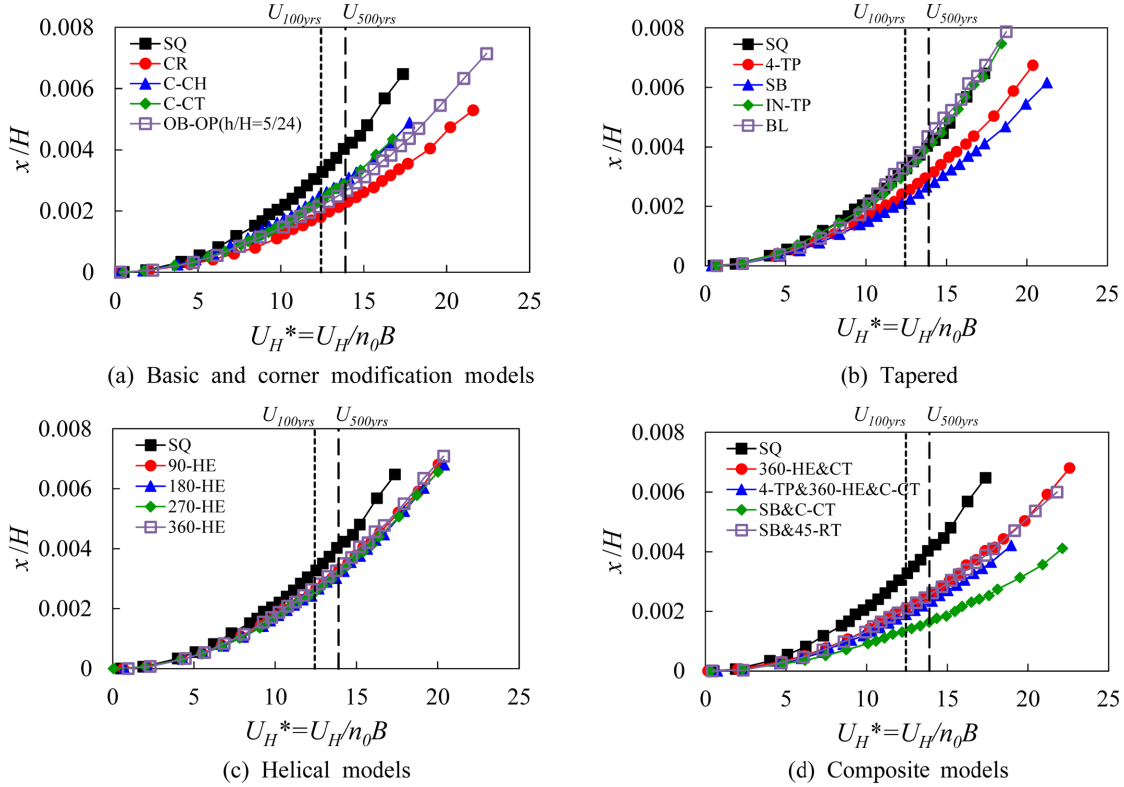
occurred. The displacement data were obtained by sampling at 300 Hz for a period, and were done for 50 samples of 10 min length in full scale conversion. Measured displacements were converted to normalized mean and standard deviation of responses at the model height.

3. Results and Discussion

3.1. Mean displacement response

Figure 4 shows variation of along-wind normalized mean displacement responses of super-tall building models with various unconventional configurations. Mean displacement responses of aerodynamically modified models are compared with those of a square model. However, across-wind mean displacement responses of super-tall building models can be neglected because these responses are close to zero. The mean displacement response of all experimental models are gradually increased with reduced wind velocities. An interesting observation was that most of super-tall building models show better aerodynamic behaviors except the inversely 4-tapered and bulged models as shown in Figure 4(b). Another interesting observation was that for helical models, there is no effect on the change of the twist angle of the helical model in the mean displacement response as shown in Figure 4(c).

Figure 5 shows along-wind mean displacement responses of super-tall building models at reduced wind velocity, 12.42 corresponding to 100-year return period wind speed. Notable observation was that composite models with multiple modifications are most effective for reducing the mean wind loads compared with those of other models with single



(a) Basic and corner modification models

(b) Tapered

(c) Helical models

(d) Composite models

Figure 4. Along-wind mean displacement responses of super-tall building models with various unconventional configurations.

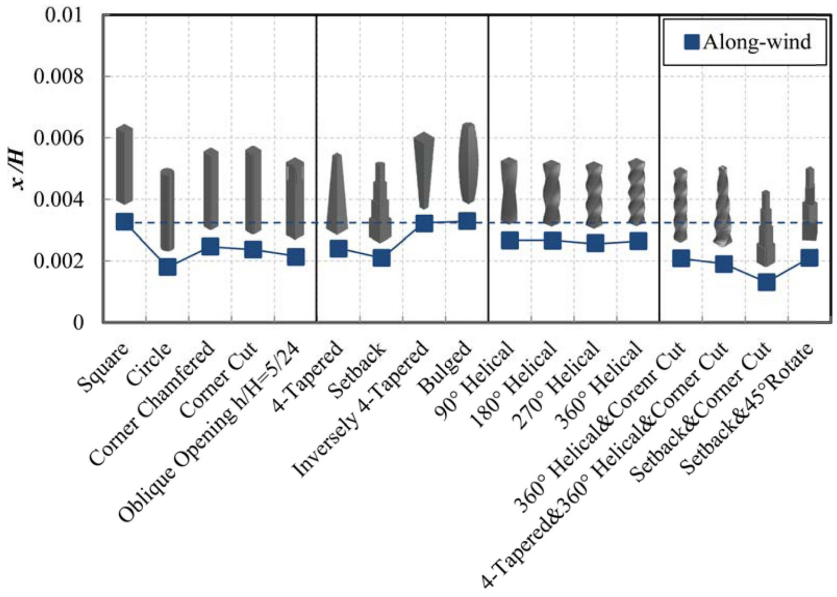


Figure 5. Comparison of mean displacement responses at 100-year return period wind speed.

modification. Particularly, the mean displacement responses of the 4-tapered and corner cut model are reduced to 60% from that of the square model as shown in Figure 4(d).

3.2. Fluctuating displacement response

Figure 6 shows variation of normalized fluctuating displacement responses of super-tall building models with various unconventional configurations in along-wind direction. The fluctuating displacement responses of aerodynamically modified models are compared with those of the square model. An interesting observation was that most of super-tall building models show better aerodynamic behaviors in along-wind fluctuating displacement response except the inversely 4-tapered models as shown in Figure 6. Along-wind RMS displacement responses of circular, setback, 180°helical, 270°helical and composite models are reduced

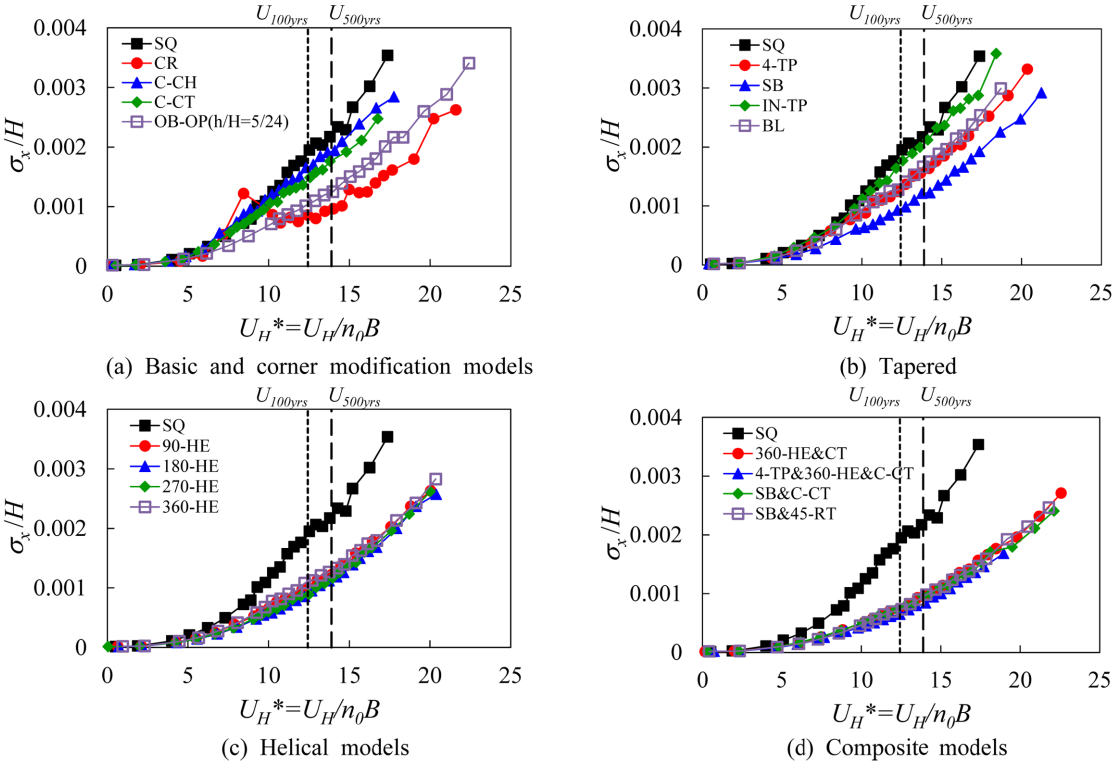


Figure 6. Along-wind fluctuating displacement responses of super-tall building models.

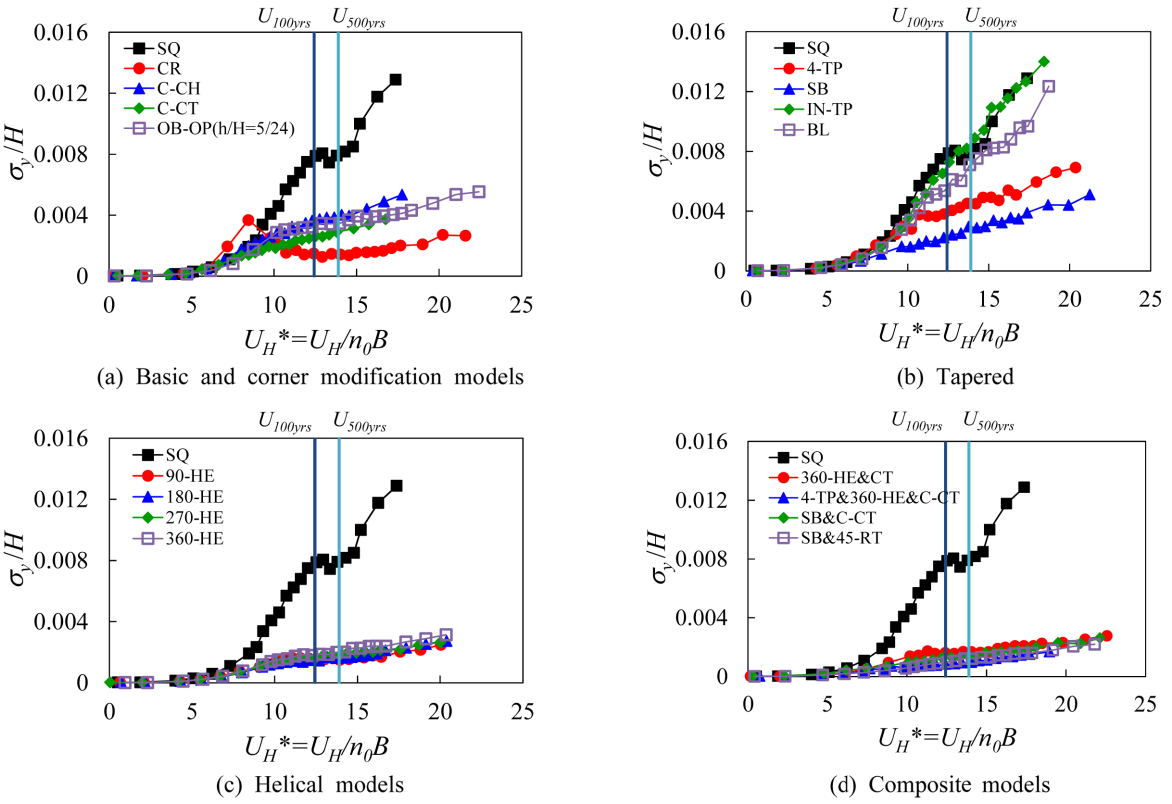


Figure 7. Across-wind fluctuating displacement responses of super-tall building models.

to over 50% from that of the square model.

Figure 7 shows variation of normalized fluctuating displacement responses of super-tall building models with various unconventional configurations in across-wind direction. The fluctuating displacement response of the square model with a reduced velocity > 17 is excluded from the experiment because it is out of the range for the measuring system. It is noticeable that the fluctuating displacement response of the square model is significantly increased over the reduced velocity of 15 due to the aerodynamic instability. On the other hand, corner modification, tapered, helical and composite models do not exhibit the aerodynamic instability at any of the reduced velocities except the in inversely 4-tapered and bulged models which are occurred the aerodynamic instability at the reduced velocity of 15.16 for inversely tapered model and of 17.4 for bugled model. Another notable observation was that circular, helical and composite models show relatively small values and similar amplitude of those of along-wind fluctuating displacement responses. It implies that circular, helical and composite models are effective in reducing the across-wind fluctuating wind loads. However, the circular model is occurred vortex shedding at reduced velocity of 8.4 as shown in Figure 7(a).

Figure 8 shows along- and across-wind fluctuating displacement responses of super-tall building models at reduced wind velocity, 12.42 corresponding to 100-year return period wind speed. As shown in Figure 8, most of aerodynamically modification models in along- and across-wind fluctuating displacement responses are smaller except the inversely tapered and bugled models whose are similar trends or slightly decrease from that of square model. Particularly fluctuating displacement responses of circular, setback, helical and composite models in both along- and across-wind directions show relatively small values. Further, the 4-tapered & 360°helical & corner cut model is most effective in reducing both along- and across-wind fluctuating displacement responses compared with all experimental models. Fluctuating displacement responses in along- and across-wind directions are decreased to 33.3% and 10.5% from those of the square model respectively. These results are in agreement with those of Tanaka et al. (2012). For single modification, helical models show good aerodynamic characteristics in both along- and across-wind fluctuating displacement responses. However, there is almost no effect of twist angle in helical models.

3.3. Power spectral density

Figure 9 presents examples of the power spectral densities of the across-wind fluctuating displacement responses of super-tall building models at reduced wind velocity, 12.42 corresponding to 100-year return period wind speed. As shown in Figure 9, the natural frequency component peaks of experimental models and the Strouhal number peaks merge at this reduced velocity, and they cannot be distinguished. A notable observation was that energies for aerodynamically modification models are small from those of

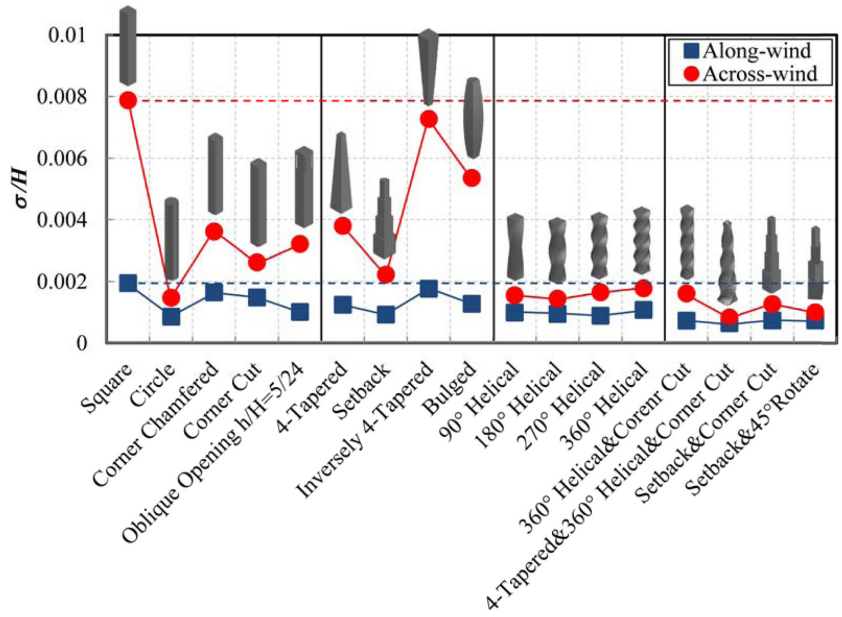
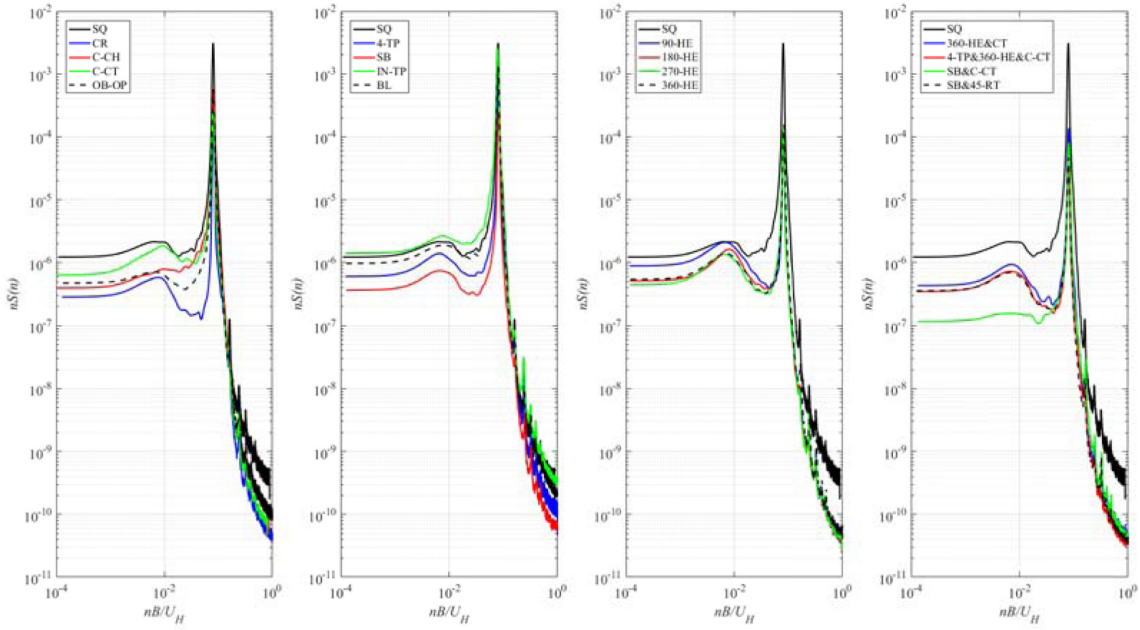


Figure 8. Comparison of fluctuating displacement responses on super-tall buildings at design wind speed.



(a) Basic models (b) Tapered models (c) Helical models (d) Composite models

Figure 9. Power spectral densities of fluctuating displacement responses on super-tall buildings at design wind speed.

square model except the inversely tapered and bulged models which are slightly higher or same with that of square model. These results are good agreement with across-wind fluctuating displacement responses at design wind speed as shown in Figure 8. It implies that regular vortex shedding mechanism of aerodynamically modification models are disintegrated, and then the mitigations of vortex shedding are effective in reducing across-wind fluctuating displacement responses (Tamura et al., 2013).

3.4. Characteristics of aerodynamic damping ratios

The aerodynamic damping of a 180° helical supertall building(180-HE), which showed good aerodynamic behavior in terms of both along- and across-wind responses as discussed in sub-section 3.2 is investigated, and compared with those of the square model. The aerodynamic damping ratio of the supertall building is evaluated using the random decrement technique (RDT) which is widely used to identify the dynamic characteristics of the structures subjected to

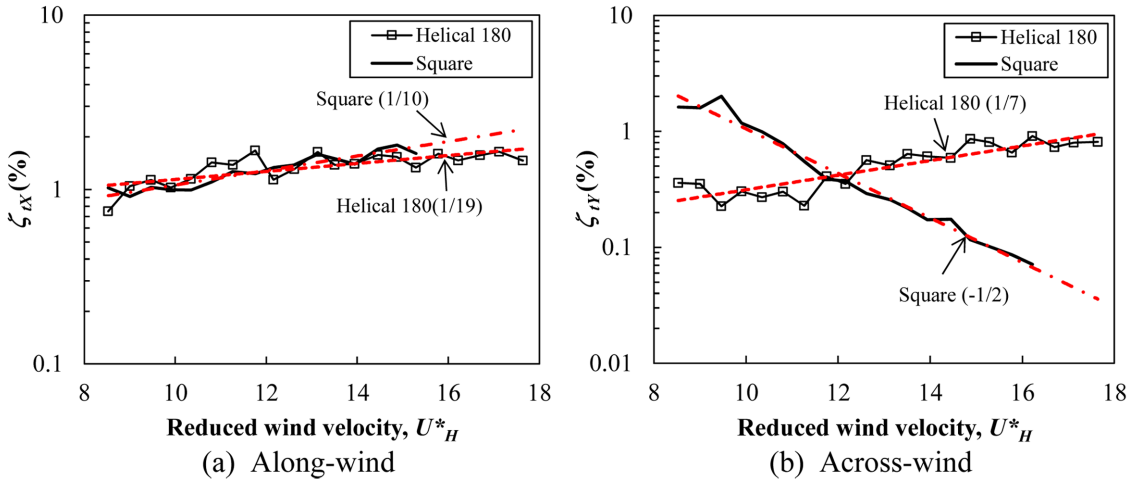


Figure 10. Relationship between reduced velocity and total damping ratios.

ambient loads as follows:

$$\alpha(\tau)=\frac{1}{N}\omega(t_i)\times(t_i+\tau)\Big|_C \quad (1)$$

where, a(t) represents the random decrement (RD) signatures, and N, $\omega(t_i)$, and C are the number of samples, weight coefficients, and triggering level for determining the time segment. In this study, the standard deviation of the displacement response was used to determine the triggering level. Superimpositions were carried out using the data extracted outside the natural frequency using a band-pass filter. The total damping ratio is obtained by using five cycles in the RD signature time history.

Figure 10 shows relationship between reduced velocity and total damping ratios in along- and across-wind directions. In the along-wind direction, total damping ratios for the square and the 180° helical models are proportional to a power of 1/10 and 1/19 (represented by the slope on the log-log plot), respectively as shown in Figure 10(a). The aerodynamic damping ratios of the 180° helical model show a similar distribution to those of the square model, and there is no clear variation in the aerodynamic damping ratio with respect to the building shape.

In the across-wind direction, the aerodynamic damping ratio of the 180° helical model is quite different from that of the square model as shown in Figure 10(b). The total damping ratio for the square model is proportional to power of -1/2. On the other hand, the total damping ratio for the 180° helical model is quite different from that of the square model, and is inversely proportional to a power of 1/7 as shown in Figure 10(b). It is obvious that the aerodynamic damping ratio of the square model rapidly decreases when the reduced velocity is > 9 and the positive aerodynamic damping ratio changes to a negative aerodynamic damping ratio. This implies that the effect of the aerodynamic damping force on the 180° helical model is almost insignificant in terms of the displacement response as shown in Figure 7(c).

4. Conclusions

The wind-induced response characteristics and aeroelastic instability of super-tall buildings with various unconventional configurations were investigated by extensive aeroelastic model experiments. The following results are obtained:

1) Corner modification, tapered, helical and composite models do not exhibit the aerodynamic instability at any of the reduced velocities except the in inversely 4-tapered and bulged models which are occurred the aerodynamic instability at the reduced velocity of 15.16 for inversely tapered model and of 17.4 for bugled model.
2) Aerodynamic characteristics of helical models with single modification are superior to those of other models with single modification. In addition, the aerodynamic characteristics have not been improved by the changing of the twist angle of helical model.
3) The 4-tapered & 360° helical & corner cut model is most effective in reducing the along- and across-wind fluctuating displacement responses in all of experimental models.

These results can be used in the preliminary design stage, and can be helpful in evaluating the most effective structural shape in wind-resistant design for tall buildings with various aerodynamic modifications.

5. Acknowledgement

This work is supported by the Korea Environmental Industry & Technology Institute(KEITI) grant funded by the Ministry of Environment(RE201901072), and by the Ministry of Education, Culture, Sports, Science and Technology, Japan, through the Joint Usage / Research Center of Wind Engineering, Tokyo Polytechnic University, 2013-2019. The authors gratefully acknowledge their support.

References

Architectural Institute of Japan (AIJ-RLB 2004), Chapter 6: Wind Loads, Recommendations for Loads on Buildings

Bandi E.K., Tanaka H., Kim Y.C., Ohtake K., Yoshida A., Tamura Y. (2013) Peak pressure acting on tall buildings with various configurations, *International Journal of High-Rise Buildings*, 2:3, 229-244.

Cooper K.R., Nakayama M., Sasaki Y., Fediw A.A., Resende-Ide S., Zan S.J. (1997) Unsteady aerodynamic force measurements on a super-tall building with a tapered cross section, *J. Wind Eng. Ind. Aerodyn*, 72, 199-212.

Davenport A.G. (1988) The response of super tall buildings to wind, Second Century of the Skyscraper, *Council on Tall Buildings and Urban Habitat*, 705-725.

Kawai H. (1998) Effect of corner modifications on aeroelastic instabilities of tall buildings, *J. Wind Eng. Ind. Aerodyn*, 74-76, 719-729.

Kim Y.C., Kanda J. (2010) Characteristics of aerodynamic forces and pressures on square plan buildings with height variations, *J. Wind Eng. Ind. Aerodyn*, 98, 449-465.

Kim Y.C., Kanda J., Tamura Y. (2011) Wind-induced coupled motion of tall buildings with varying square plan with height, *J. Wind Eng. Ind. Aerodyn*, 99, 638-650.

Kim Y.M., You K.P., (2002) Dynamic responses of a tapered tall building to wind load, *J. Wind Eng. Ind. Aerodyn*, 90, 1771-1782.

Kwok, K.C.S., Wilhelm, P.A., Wilkie, B.G. (1988) Effect of edge configuration on wind-induced response of tall buildings, *Engng. Struct*, 10, 135-140.

Tamura Y., Kim Y.C., Tanaka H., Bandi E.K., Yoshida A., Ohtake K. (2013) "Aerodynamic and responses characteristics of super-tall buildings with various configuration", Proc. 8th Asia-Pacific Conference on Wind Engineering, December 10-14, 2013, Chennai, India

Tamura Y., Nakai M., Ohtake K., Koshika K., Yamawaki K. (2011) Study on wind resistant design method of super high-rise buildings with various unconventional configurations, The Minisitry of Land, Infrastructure, Transport and Tourism, Tokyo, Japan (in Japnaese).

Tanaka H., Tamura Y., Ohtake K., Nakai M., Kim Y.C. (2013) Aerodynamic and flow characteristics of tall Buildings with various unconventional configurations, *International Journal of High-Rise Buildings*, 2:3, 213-228.

Tanaka H., Tamura, Y., Ohtake K., Nakai, M., Kim, Y. C. (2012) Experimental investigation of aerodynamic forces and wind pressures acting on tall buildings with various unconventional configurations, *J. Wind Eng. Ind. Aerodyn*. 107-108, 179-191.